

Soft-X-Ray Absorption Spectra and Core-Threshold Behavior in the Alkali Metals

E. Zaremba

Department of Physics, Queen's University at Kingston, Kingston, Ontario, Canada K7L 3N6

K. Sturm

Institut für Festkörperforschung, Forschungszentrum Jülich GmbH, D-5170 Jülich, Germany

(Received 28 November 1990)

We have calculated the nonlocal dielectric function of the alkali metals in the region of the p -core excitation threshold. The theory is at the level of the random-phase approximation and includes the self-consistent response of both valence and core electrons. We find that the peaking of threshold absorption is due to valence-electron-hole excitations which are induced by the dynamic dipole field of the core electrons. Our results are in good agreement with experiment and offer an alternative explanation of threshold behavior to that provided by the Mahan-Nozières-de Dominicis theory.

PACS numbers: 78.70.Dm, 71.45.Gm, 78.20.Bh

The soft-x-ray spectra of many simple metals are characterized by a prominent peak at p -core excitation thresholds. Such structure is commonly attributed to the edge singularities which emerge from the Mahan,¹ Nozières, and de Dominicis² (MND) theory.³ The theory has provided a qualitative explanation for much of the experimental data but in some cases, when examined in more critical detail, it has been found to be deficient. For example, Bruhwiler and Schnatterly⁴ have recently come to the conclusion that the MND theory does not give a consistent explanation of the x-ray absorption, emission, and photoemission data of sodium and potassium. Thus, although the MND theory has provided a rationale for threshold peaking, it cannot be claimed to have been thoroughly vindicated.

In this Letter, we discuss threshold behavior from a more conventional point of view, namely, in terms of the dielectric-response function calculated at the level of a self-consistent-field approximation. Our intention is to show that many of the experimental features are apparent even within this theory. More importantly, the threshold behavior is placed in the context of the total x-ray absorption associated with core excitations extending to energies well above threshold. While those aspects addressed by the MND model are no doubt relevant, there are other physical effects, at least of equal importance, which must be included if a complete understanding of the data is to be achieved.

Before describing the content of our theory, we briefly summarize, for purposes of comparison, the essential features of the MND model.³ Ultimately, threshold singularities arise because of a sharp Fermi cutoff which leads to the appearance of a logarithmic singularity at threshold in the bare core-electron dynamic polarizability. As first shown by Mahan,¹ the repeated interaction of the valence electrons with the created core hole constitutes an excitoniclike response which compounds the logarithmic singularity into an algebraic one. Subsequent-

ly, Nozières and de Dominicis² (ND) presented a more complete analysis which, in addition to Mahan's considerations, also included the Anderson orthogonalization effect. The ND formalism made it clear that the dynamics of the core hole did not play an essential role in the model being considered and that the response of the (noninteracting) valence electrons to a localized time-dependent perturbation was responsible for the final spectrum.

Several complicating factors are known to exist,³ such as core-hole lifetimes, phonons, finite temperature, core-level degeneracies, core-valence exchange, and valence-electron interactions. The last, in particular, is believed not to alter the calculated singular behavior in any essential way. However, conclusions of this kind are again based on considerations of the MND model in which the calculation of the x-ray absorption is restricted to real core excitations and in which electron-electron interactions are included only within the core-hole-valence-electron channel. In reality, core-electron excitations occur in concert with dynamic charge fluctuations which couple to all electrons, core and valence alike. It is the importance of these effects which we wish to emphasize here.

In a previous paper,⁵ we formulated a theory of the dielectric response of simple metals which included core polarization and examined its effect on the plasma frequency. The theory was based on the random-phase approximation (RPA) and treated the response of both core and valence electrons on an equal footing. The essential physical idea is that polarization of the ionic core gives rise to dipolar fields which couple to the valence electrons. Thus the total response of the metal to an external perturbation is determined by the self-consistent interaction between these two groups of electrons.

With the simplifying approximations adopted in Ref. 5, the dielectric function takes the form

$$\epsilon(\omega) = \epsilon_c(\mathbf{q} \rightarrow 0, \omega) + \frac{4\pi n_i \alpha(\omega)}{1 - (4\pi/3)n_i \alpha(\omega) \{1 + \sum_{\mathbf{G} \neq 0} f(\mathbf{G}, \omega) [1 - 1/\epsilon_c(\mathbf{G}, \omega)]\}} \quad (1)$$

Here $\epsilon_r(\mathbf{q}, \omega)$ is the valence-electron dielectric function calculated in the nearly-free-electron pseudopotential approximation; local-field effects associated with inhomogeneities in the valence-electron system are neglected. The second term, to be denoted $\epsilon_{CM}(\omega)$, is of the Clausius-Mossotti form and arises from the polarization of the core electrons as characterized by the core polarizability $\alpha(\omega)$. The denominator accounts for the usual lattice local-field effects; however, an essential modification appears in the form of the sum over reciprocal-lattice vectors \mathbf{G} . The latter is due to the response of the valence electrons to the periodic potential produced by the core dipole moments. The function $f(\mathbf{G}, \omega)$ is proportional to the Fourier transform of the induced core-electron charge fluctuation and can be referred to as a dipole form factor. The remaining parameter in Eq. (1) is the atomic volume density n_i .

The interesting features of $\epsilon(\omega)$ in the vicinity of the core excitation threshold ω_T are due to the behavior of the core polarizability $\alpha(\omega)$. The latter is calculated taking into account Coulomb interactions between the core electrons. As mentioned previously, the *noninteracting* core polarizability $\alpha_0(\omega)$ exhibits a logarithmic singularity at $\omega = \omega_T$ because of the sharp Fermi cutoff. Although the singularity is modified when core-electron interactions are treated self-consistently, it still leads to a pronounced peak in $\text{Re}\alpha(\omega)$ at threshold. This, in turn, leads to sharp features in both $\text{Re}\epsilon_{CM}(\omega)$ and $\text{Im}\epsilon_{CM}(\omega)$ which can be identified with the threshold behavior observed.

We have performed calculations of the dielectric function using Eq. (1) for the alkali metals Na, K, Rb, and Cs. In Fig. 1, we show $\epsilon_1(\omega)$ and $\epsilon_2(\omega)$ for the case of K. A comparison of $\epsilon_1(\omega)$ with the corresponding experimentally derived quantity⁴ demonstrates that the theoretical results are in good qualitative agreement. The one notable discrepancy concerns a shift of the $3p$ excitation threshold from the experimental value of 18.3 eV to the calculated value of 15.8 eV. This is related to the inherent limitation of the local-density approximation⁶ which underestimates core-electron binding energies. Were it not for this shift, the theoretical results for $\epsilon_1(\omega)$ would clearly be in quantitative agreement with experiment. The other noticeable difference is the lack of small-scale structure in the theoretical curve. This is due to our approximate treatment of the metallic lattice; outside the core region, the metal is represented as a uniform electron gas. As a result, we do not include the Bloch-state nature of the excited states which imparts features of the band structure to the core polarizability. It is nevertheless clear that the overall spectral response follows closely the experimental results.

The sharp peak at threshold seen in both $\epsilon_1(\omega)$ and $\epsilon_2(\omega)$ arises from the corresponding peak in $\alpha(\omega)$. Only a single peak appears since we have neglected the spin-orbit splitting of the core levels in the underlying electronic structure. In order to make a more detailed com-

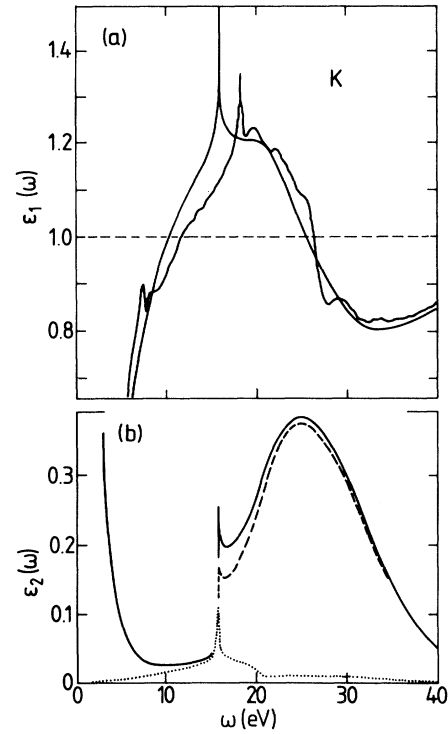


FIG. 1. (a) Real and (b) imaginary parts of the dielectric function of potassium as a function of frequency in the vicinity of the $4p$ threshold. The smooth curve in (a) is theory, the other is from Ref. 4. The decomposition of $\text{Im}\epsilon_{CM}(\omega)$ is shown in (b): direct core absorption (dashed line) and core-induced valence absorption (dotted line).

parison with experiment, we will later introduce spin-orbit splitting in a semiempirical way. However, before doing so, we examine the origin of the peak behavior in $\text{Im}\epsilon_{CM}(\omega)$. Denoting the sum over \mathbf{G} in Eq. (1) by $\lambda(\omega) = \lambda_1(\omega) + i\lambda_2(\omega)$, we have

$$\text{Im}\epsilon_{CM}(\omega) = \frac{4\pi n_i \alpha_2(\omega) + |4\pi n_i \alpha(\omega)|^2 \lambda_2(\omega)/3}{|1 - (4\pi/3)n_i \alpha(\omega)[1 + \lambda(\omega)]|^2}. \quad (2)$$

This makes clear that there are two distinct contributions to the absorption near threshold. The first term in the numerator of Eq. (2) is proportional to $\alpha_2(\omega)$ which is only finite for $\omega \geq \omega_T$. This term corresponds to the direct excitation of core electrons, modified of course by local-field effects as represented by the denominator. The second contribution is due to $\lambda_2(\omega)$ which is finite even below threshold. In this frequency range, its interpretation is particularly clear: $\lambda(\omega)$ has an imaginary part only because of the imaginary part of $\epsilon_r(\mathbf{G}, \omega)$ which, for the \mathbf{G} and ω values of interest, is due to valence-electron-hole excitations. In addition, the second contribution contains the factor $|\alpha(\omega)|^2$ which is proportional to the square of the amplitude of the induced core dipole moment. In other words, the oscillatory field of the core dipole moment is the agent exciting

electron-hole pairs within the valence-electron system. In Fig. 1(b), we illustrate the decomposition of $\text{Im}\epsilon_{\text{CM}}$ into these two contributions. It is clear that electron-hole excitations make an important contribution near threshold and, more significantly, that this contribution is sharply peaked at $\omega = \omega_T$ because of the enhanced magnitude of the core dipole moments. Most of the peaked structure in $\epsilon_2(\omega)$ at threshold is due to this electron-hole pair contribution. This mechanism for absorption is not contained within the MND model.

The actual threshold behavior of Na and K exhibits a double-peaked structure because of spin-orbit splitting.⁴ In order to make a more detailed comparison of our theoretical results with experiment, we have attempted to include this effect, together with broadening, in an approximate way. We assume that the core polarizability with spin-orbit splitting is simply a superposition of two components with the appropriate spin-orbit weighting, i.e., $\text{Im}\bar{\alpha}(\omega) = w_1 \text{Im}\alpha(\omega) + w_2 \text{Im}\alpha(\omega - \Delta_{\text{s.o.}})$, where $\alpha(\omega)$ is the calculated polarizability without spin-orbit splitting, w_1 and w_2 are the spin-orbit weights, and $\Delta_{\text{s.o.}}$ is the spin-orbit energy. By the Kramers-Kronig formula, the real part satisfies a similar relation. Each of the spin-orbit components is then separately convoluted with a Gaussian of width σ_1 and σ_2 , respectively. The final result for K is shown in Fig. 2(b) which is to be compared with the experimental result⁴ in Fig. 2(a). The two results are very similar and it is clear that the threshold peak in Fig. 1(b) accounts for a significant part of the experimental structure. We note that the ex-

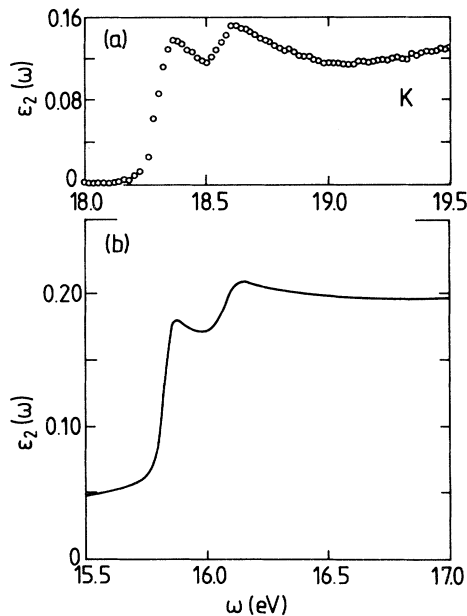


FIG. 2. The threshold behavior of $\epsilon_2(\omega)$ of potassium: (a) experiment from Ref. 4; (b) theory. The theoretical curve is calculated with the following parameters (see text): $\Delta_{\text{s.o.}} = 0.25$ eV, $w_1 = 0.71$, $w_2 = 0.29$, $\sigma_1 = 0.03$ eV, $\sigma_2 = 0.05$ eV.

perimental curve is obtained by subtracting a background to isolate the core excitation component. As explained previously, such a procedure is not too meaningful since the threshold behavior in our picture is a superposition of core and valence contributions. Nevertheless, if we subtract a constant background of 0.05 from our theoretical result, the remaining magnitude is then in quantitative agreement with experiment. We emphasize that a quantitative comparison at this level has never been attempted previously.

We finally consider the absorption coefficient defined by

$$\mu(\omega) = \omega \epsilon_2(\omega) / n(\omega) c = 4\pi \text{Re}\sigma(\omega) / n(\omega) c, \quad (3)$$

where $n(\omega)$ is the refractive index and $\sigma(\omega)$ is the conductivity. The upper panel in Fig. 3 shows the experimental data⁷ for K, Rb, and Cs while the lower panel contains the theoretical results including spin-orbit splitting. The overall structure and relative magnitudes of the absorption coefficients for the various metals are very well reproduced. The absolute magnitude of the absorption is in somewhat poorer agreement, with theory consistently overestimating μ by 50%. However, it is difficult to obtain an accurate absolute measure of the absorption and it is conceivable that there are errors in the experimental results. Indeed, Bruhwiler and Schnatter-

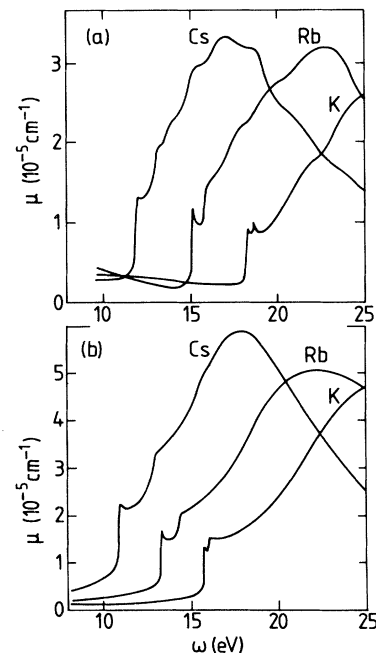


FIG. 3. Absorption coefficient μ vs frequency for K, Rb, and Cs: (a) experiment from Ref. 7; (b) theory. The parameters for K are the same as in Fig. 2. The parameter set for Rb is $\Delta_{\text{s.o.}} = 1.0$ eV, $w_1 = \frac{2}{3}$, $w_2 = \frac{1}{3}$, $\sigma_1 = 0.02$ eV, $\sigma_2 = 0.15$ eV, while the set for Cs is $\Delta_{\text{s.o.}} = 1.84$ eV, $w_1 = \frac{2}{3}$, $w_2 = \frac{1}{3}$, $\sigma_1 = 0.05$ eV, $\sigma_2 = 0.15$ eV.

ly⁴ have already noted discrepancies between data obtained by different techniques which points to uncertainties in the measured absorption coefficients. The relatively good agreement with experiment we obtain for $\epsilon_1(\omega)$, as shown in Fig. 1(a), at least suggests that our theoretical values for the absorption coefficient of K are reliable in the energy range 20–40 eV.

It is of interest to note that the position of the peaks in the absorption coefficients are given correctly by theory in spite of the discrepancies in the threshold positions. The main part of the oscillator strength of the optical transitions is a collective response of the core which is well described by the self-consistently calculated core polarizability. The threshold position, however, is tied to the position of the core level which, as already mentioned, is too shallow in the local-density approximation. As a result, there appears to be a distortion of the calculated absorption spectra associated with the displacement of threshold away from the higher-energy maximum. It is particularly clear in the case of K that an upward shift of the calculated threshold by 2.5 eV would bring theory closely in line with experiment. It is not known whether this has any bearing on the slightly different behavior seen in $\epsilon_2(\omega)$ in Fig. 2 in the range 1–2 eV above threshold.

We should at this point indicate some of the limitations of our analysis. We refer to Ref. 5 for a more detailed discussion of the approximations made in the derivation of Eq. (1). Perhaps the most significant approximations in the present context are those associated with the valence dielectric matrix $\epsilon_{GG'}^v(\omega)$. First, this matrix was replaced by its diagonal components which effectively eliminates local-field effects within the valence-electron system. To the extent that the dipolar-induced valence excitations are of primary interest [see the second term in Eq. (2)], this is probably not an overwhelmingly important effect. More significant is the use of the Lindhard function to estimate $\epsilon_r(\mathbf{G}, \omega)$ appearing in the denominator of Eq. (1), modified in a way to ensure the satisfaction of the f -sum rule. The dipole-induced valence-electron transition rates are nevertheless effectively calculated using plane-wave states, rather than the correct Bloch states. The use of the latter will clearly affect the amplitude of $\lambda_2(\omega)$ in Eq. (2). It would therefore be of interest to introduce these refine-

ments in future calculations.

Another consideration is the importance of the particle-hole interactions retained in the MND model. In principle, these could be included to yield an improved approximation for the proper polarization that supercedes the use of the noninteracting density-response function within the RPA theory. However, this would appear to be extremely difficult to carry out if some semblance of reality is to be retained in the description of the core-electronic structure. Furthermore, if one is interested in the actual core dipole moment and the spatial distribution of the induced core charge, the explicit Coulomb nature of the electron-hole interactions must be preserved. These are all complications which at some point must be addressed.

In conclusion, we have performed detailed calculations of the soft-x-ray absorption spectra of the alkali metals which compare favorably with the available experimental data. Within the framework of an RPA theory, threshold peaking arises as a result of valence-electron excitations induced by the oscillating core dipole moments. These effects are not included within the MND theory and are clearly essential for a complete understanding of threshold behavior in the simple metals.

This work was supported in part by a grant from the Natural Sciences and Engineering Research Council of Canada. One of us (E.Z.) acknowledges the hospitality of the Max-Planck-Institut für Festkörperforschung, Stuttgart.

¹G. D. Mahan, Phys. Rev. **163**, 612 (1967).

²P. Nozières and C. T. de Dominicis, Phys. Rev. **178**, 1084 (1969).

³For a comprehensive review, see C. O. Almbladh and L. Hedin, in *Handbook on Synchrotron Radiation*, edited by E. E. Koch (North-Holland, Amsterdam, 1983), Vol. 18, p. 607.

⁴P. A. Bruhwiler and S. E. Schnatterly, Phys. Rev. B **41**, 8013 (1990).

⁵K. Sturm, E. Zaremba, and K. Nuroh, Phys. Rev. B **42**, 6973 (1990).

⁶P. Hohenberg and W. Kohn, Phys. Rev. **136**, B964 (1964); W. Kohn and L. J. Sham, Phys. Rev. **140**, A1133 (1965).

⁷S. Sato, T. Miyahara, T. Hanyu, S. Yamaguchi, and T. Ishii, J. Phys. Soc. Jpn. **47**, 836 (1979).